ORIGINAL ARTICLE

Mesoporous Cyclodextrin nanosponges-based Formulation for the Effective Buccal Delivery of Curcumin

Praveen Gujjula[1], AngalaParameshwari[2]

[1]Department of Pharmaceutical Sciences, Jawaharlal Nehru Technological University, Ananthapuramu, Andhra Pradesh, India, [2]Department of Pharmaceutical Analysis, Ratnam Institute of Pharmacy, Nellore, Andhra Pradesh, India.

ABSTRACT

Background: Curcumin (CUR), a bioactive compound from Curcuma longa, has limited clinical utility due to poor solubility and low oral bioavailability. To overcome these challenges, this study developed mesoporous cyclodextrin nanosponge (CDNS)-based buccal tablets designed for enhanced, bioadhesive, and sustained curcumin delivery. **Materials and Methods:** Nanosponges (NSs) were synthesized through cross-linking and loaded with curcumin by freeze-drying. Buccal tablets were prepared by direct compression and optimized using Box-Behnken design. Characterization included particle size analysis, Fourier-transform infrared spectra, X-ray diffraction, differential scanning calorimetry, and evaluation of tablet physical properties, mucoadhesion, swelling, surface pH, *in vitro* drug release, and stability. **Results:** Curcumin-loaded NSs (95–139 nm) were smaller than plain NSs (140–180 nm) and exhibited low polydispersity with 20–35% drug loading. Spectroscopic and thermal analyses confirmed successful inclusion complex formation. Optimized tablets containing hydroxypropyl methylcellulose K4M (16.59%), Carbopol 934 (9.91%), and Chitosan (14.49%) showed acceptable physicochemical and mucoadhesive properties. *In vitro* studies demonstrated sustained curcumin release superior to the pure drug. Stability remained consistent over time. **Conclusion:** Mesoporous CDNS-based buccal tablets significantly improved curcumin's solubility, mucoadhesion, and controlled release, representing a promising formulation for enhanced buccal drug delivery.

Key words: Design of experiments, drug permeability, inclusion complex, mucoadhesion, nanosponges, sustained release

INTRODUCTION

Curcumin (CUR), a bioactive compound derived from turmeric, exhibits a broad spectrum of pharmacological activities, including antioxidant, anti-inflammatory, and anticancer effects. However, its clinical application is limited by poor aqueous solubility, rapid metabolism, and a short biological half-life (1–2 h in humans).[1-3] The pharmacokinetics of CUR are influenced by several factors, such as formulation type, dosage, and route of administration. To address the challenges of low bioavailability and limited systemic retention, various advanced delivery systems such as nanoparticles, liposomes, and phospholipid complexes have been developed to enhance the solubility, stability, and therapeutic efficacy of CUR.[4,5]

Cyclodextrin-based nanosponges (CDNS) have emerged as promising carriers for the delivery of poorly soluble drugs. Cyclodextrins (CDs), with their hydrophobic cavity and hydrophilic exterior, have been widely used to encapsulate hydrophobic compounds.[6] While first-generation CD systems faced challenges with solubility and stability,[7] subsequent generations, especially CDNS formed through cross-linking, offer improved porosity, stability, and drug-loading capacity.[8] CDNS have been successfully applied to deliver a range of therapeutic agents, including anticancer, antifungal, and antibiotic drugs, enhancing bioavailability, stability, and controlled

Address for correspondence:
Praveen Gujjula,
Department of Pharmaceutical Sciences, Jawaharlal Nehru Technological University, Ananthapuramu, Andhra Pradesh, India.
E-mail: praveen.pharma33@gmail.com

Received: 23-08-2025
Revised: 25-09-2026
Accepted: 30-09-2025

release.[9-11] In particular, curcumin (CUR)-loaded CDNS have demonstrated improved solubility, sustained release, and increased cytotoxicity against cancer cells.[12,13] Their potential in buccal drug delivery is also notable, with studies showing enhanced mucoadhesion, permeation, and pharmacokinetic profiles when incorporated into films or patches.[14,15] Overall, CDNS represent a versatile platform for developing advanced drug delivery systems across multiple routes of administration.[16]

Buccal drug delivery offers significant benefits, including avoidance of first-pass metabolism, rapid onset, and ease of administration.[17,18] Dosage forms, such as tablets, films, gels, and patches provide mucoadhesion and sustained release, making this route effective for both systemic and local therapies.[19,20] Although limited by a small absorption area, advances, such as CD-based nanosponges (CDNS) have enhanced solubility, bioavailability, and mucosal retention.[21,22] In the case of curcumin, buccal formulations have shown improved bioavailability and sustained release over oral delivery,[23,24] yet challenges of mucoadhesion, stability, and taste masking persist,[25] supporting the exploration of CDNS as a novel buccal carrier for CUR.

Polymer selection is critical in buccal tablet formulation to achieve mucoadhesion and controlled drug release. Hydroxypropyl methylcellulose (HPMC® K4M) provides strong adhesion, gel formation, and sustained release,[27,28] while Carbopol® 934 enhances mucoadhesion and modulates release through concentration adjustment.[29,30] Chitosan further improves adhesion and facilitates drug permeation.[31] Their combination offers synergistic benefits – extended release, improved retention, and enhanced absorption – highlighting the need for careful optimization of polymer type and concentration.[26]

The Box-Behnken design (BBD) construct is a way to construct tests that look at numerous elements and how they interact with each other in fewer experiments. The reason for choosing BBD for nanosuspension development is that it can give a balanced analysis of three or more elements with fewer experimental runs than complete factorial designs. BBD has a lot of benefits, such as cutting down on the number of trials, saving time and money, and giving more reliable data for optimization. BBD can also accurately forecast the best formulation based on the effects of each factor and how they work together. This makes it the best choice for the complicated process of creating nanosponges (NSs).

MATERIALS AND METHODS

Materials

Curcumin (CUR), β-Cyclodextrin (β-CD), chitosan, dimethyl sulfoxide (DMSO), and magnesium stearate were procured from Sigma-Aldrich Chemicals Pvt. Ltd. Carbopol 934, HPMC K4M, and diphenyl carbonate (DPC) were obtained from HiMedia Laboratories (Thane, India). Ethanol and methanol were supplied by SD Fine Chem Ltd. (Hyderabad, India). Milli-Q water was used throughout the study.

Methods

CDNS crosslinking

Cyclodextrin-based nanosponges (CDNS) were synthesized using DPC as a crosslinker following a reported method.[32] Anhydrous β-cyclodextrin (β-CD) was dissolved in anhydrous DMSO, reacted with DPC at 90°C for 6 h under reflux, and purified by water washing and Soxhlet extraction with ethanol. The dried product was ground, dispersed in water, and freeze-dried to obtain NS powder. Five variants (NS1-NS5) were prepared by varying DPC/β-CD molar ratios, and their curcumin solubilization efficiencies were assessed.

CU loading into CDNS

Curcumin was loaded into CDNS using a freeze-drying method. CDNS were dispersed in 50 mL Milli-Q water with excess CUR, followed by 10 min of sonication and 24 h of stirring. After centrifugation at 2,000 rpm for 10 min, the supernatant containing complexed CUR was collected and freeze-dried at −20°C under 13.33 mbar. The dried product was stored appropriately, and drug loading efficiency was calculated using a standard formula.[33]

Characterization of CDNS and CUNS

Particle size and zeta potential of CDNS and CUNS were measured using dynamic light scattering (DLS). Morphology was examined by transmission electron microscopy (TEM) at ×72,000 magnification. Fourier-transform infrared (FTIR) spectra of β-CD, CDNS, CU, physical blends (API:β-CD and API: CDNS, 1:1), and CUNS were recorded. X-ray diffraction (XRD) analysis was performed using a Huber Guinier camera (2.5°–60° 2θ) on the same samples. Thermal properties were assessed by differential scanning calorimetry (DSC). These analyses characterized the physicochemical properties and interactions of the materials.

Experimental design - Buccal tablets

Design of experiments (DOE) is employed to identify and optimize critical formulation factors influencing buccal tablet quality.[34] Response surface methodology (RSM) enables evaluation of relationships between independent and dependent variables through second-order polynomial models, capturing linear, quadratic, and interaction effects.[35] In this study, the BBD, a three-level RSM, was selected for its efficiency in assessing formulation variables with fewer runs compared to full factorial designs. BBD uses an orthogonal array to generate uniformly distributed experimental points

within the design space, with trials conducted at the midpoints of cube edges and replicates at the center to ensure reliability. This approach reduces experimental effort while effectively determining optimal formulation conditions.[36,37]

Preliminary trials identified the independent variables as HPMC K4M (A), Carbopol 934 (B), and chitosan (C), with dependent responses including Y1 (disintegration time in artificial saliva), Y2 (disintegration time in water), Y3 (swelling capacity), Y4 (dissolution), Y5 (peak detachment force), and Y6 (permeability). A BBD with 17 runs (12 factorial and 5 center points) was employed, and data were analyzed using Design-Expert v13.0.5.0. RSM was applied to model variable interactions and optimize responses, with model selection based on R^2, adjusted R^2, model *P*-value, lack-of-fit *P*-value, and coefficient of variation. Insignificant terms ($P > 0.005$) were excluded, and the relationships were represented by mathematical equations, supported by 2D contour and 3D surface plots [Table 1].

Preparation and evaluation of buccal tablets

Buccal tablets containing CUR nanosponges (CURNS) were prepared by direct compression. A 100 mg portion of lyophilized CURNS, along with excipients, was accurately weighed, blended, lubricated with magnesium stearate, and compressed into 500 mg tablets (8 mm diameter) using a tablet press. The tablets were stored in airtight, light-protected containers until evaluation. Physicochemical and biopharmaceutical characterizations were performed to assess quality, safety, and efficacy. Weight variation was determined on 20 tablets relative to the mean weight. Tablet thickness was measured using a Vernier caliper, hardness with a Monsanto tester, and friability by tumbling in a friabilator, expressed as percentage weight loss. Disintegration time was evaluated in both water and artificial saliva. Surface pH was determined by placing an electrode on the moistened tablet surface and recording the stabilized reading after 1 min.

Swelling behavior

The swelling behavior of the formulations was evaluated to assess water uptake and predict mucoadhesive potential.[38] Three tablets from each batch were weighed (W_1) and individually placed in 5 mL of phosphate buffer (pH 6.8). At pre-determined intervals (1, 2, 4, and 8 h), tablets were removed, blotted to eliminate excess surface fluid, and

Table 1: Factors and related responses

Run	A (%w/w)	B (%w/w)	C (%w/w)	R1 (min)	R2 (min)	R3	R4 (min)	R5 (N)	R6 (%)
1	15	10	0	178.54	154.86	4.73	839.58	0.49	2.73
2	15	5	7.5	159.76	163.47	5.69	1387.56	2.39	9.38
3	10	5	15	78.78	70.43	5.92	1567.84	4.23	15.65
4	15	10	15	118.54	129.76	8.98	1138.72	3.97	16.38
5	15	5	7.5	149.76	169.24	5.23	1476.86	2.64	9.72
6	20	5	15	44.75	52.97	9.23	543.28	3.75	14.64
7	15	5	7.5	156.98	167.87	5.36	1423.65	2.47	9.56
8	15	5	7.5	153.12	169.12	5.09	1408.78	2.53	9.29
9	15	0	0	35.64	3.42	2.34	889.56	0.72	1.34
10	10	10	7.5	143.12	148.73	5.98	2097.33	1.97	10.76
11	10	5	0	92.45	67.67	1.76	987.56	0.55	1.96
12	20	5	0	37.85	25.78	4.77	489.14	0.43	1.57
13	10	0	7.5	99.43	76.12	2.03	1862.32	2.17	8.38
14	20	0	7.5	15.68	23.12	6.23	1479.12	2.06	7.89
15	15	0	15	98.65	87.56	7.03	1256.76	4.32	14.54
16	20	10	7.5	132.12	143.56	7.86	934.12	1.89	10.13
17	15	5	7.5	155.43	160.56	5.78	1459.65	2.43	9.87
Mean				108.86	106.72	5.53	1249.52	2.29	9.05
Std.Dev.				3.28	4.87	0.2835	33.96	0.0967	0.2617
Observed R^2				0.9982	0.9970	0.9922	0.9973	0.9974	0.9987
Adjusted R^2				0.9959	0.9931	0.9822	0.9938	0.9942	0.9971
Predicted R^2				0.9912	0.9674	0.9455	0.9826	0.9806	0.9882
Adeq Precision				64.9346	42.5881	34.4412	62.5756	51.4254	76.5645
C.V. (%)				3.01	4.56	5.13	2.72	4.21	2.89

reweighed (W_2). The swelling index was calculated using the following equation:

$$Swelling\ index = \frac{W_2 - W_1}{W_1} \times 100 \quad (1)$$

Bio-adhesion test

Porcine buccal mucosa was excised post-slaughter and preserved in Tyrode solution at 25°C until use. The mucoadhesive strength of buccal tablets was measured by a modified balance method using mucosal strips.[39] A 1 cm mucosal patch was mounted on the upper glass vial, hydrated with Tyrode solution at 37°C for 10 min, and aligned against a tablet fixed to the lower vial with double-sided tape. Weights were incrementally added (0.5 g) until detachment occurred, and the total weight required was recorded as the mucoadhesive strength.

Determination of ex vivo residence time

The *ex vivo* residence time of buccal tablets was evaluated using a modified United States Pharmacopeia (USP) disintegration apparatus containing 900 mL phosphate buffer (pH 6.8) maintained at 37 ± 1°C. Cow buccal mucosa was fixed vertically to a wooden scale, and the formulation, pre-moistened with buffer, was applied to the mucosal surface. The apparatus allowed alternate immersion and withdrawal of the tablet, and the detachment time from the mucosa was recorded in triplicate.

Dissolution study

Dissolution studies were performed using a USP type-II apparatus in 900 mL phosphate buffer (pH 6.8) at 37 ± 0.5°C and 50 rpm. Aliquots (5 mL) were withdrawn at pre-determined intervals, replaced with fresh medium, filtered, and analyzed at 424 nm using ultraviolet spectrophotometry. Drug release data were fitted to various kinetic models, and the best-fit model was selected based on regression coefficient (R^2) values.[40,41]

Stability study

Stability studies were conducted on CUR tablets stored in amber bottles under different conditions: 25 ± 2°C/60 ± 5% RH, 30 ± 2°C/65 ± 5% RH, and 40 ± 2°C/65 ± 5% RH. Tablets were periodically examined for physical appearance, hardness, drug content, and 24-h dissolution to evaluate stability.[42]

Statistical evaluation

Results were expressed as mean ± standard deviation. Statistical analysis of mucoadhesive strength across batches was performed using one-way analysis of variance (ANOVA) followed by Tukey's *post hoc* test. A $P < 0.05$ was considered statistically significant.

RESULTS AND DISCUSSION

Preparation and characterization of CDNS

Mesoporous cyclodextrin nanosponges (CDNS) are promising carriers for buccal delivery due to their high surface area, porosity, and ability to enhance curcumin (CU) stability, solubility, and bioavailability. They also provide sustained release and improved permeation, supporting applications in oral disorders such as lichen planus and cancers. CDNS were synthesized by cross-linking β-cyclodextrin (β-CD) with DPC at five molar ratios (1:2, 1:4, 1:6, 1:8, 1:10) and characterized for uniformity before use. DLS revealed that CDNS had an average particle size of 130–180 nm with low PDI, confirming homogeneity. Zeta potential values indicated good stability and reduced risk of agglomeration. All CDNS formulations (NS1–NS5) significantly enhanced CUR solubility compared to plain CUR (87.5 µg/mL). Notably, NS2 (1:4 molar ratio) showed the highest solubilization efficiency (978.65 µg/mL), attributed to inclusion complex formation and entrapment within the NS matrix.

Preparation and characterization of CURNS

CUR was loaded into all five NS variants using the freeze-drying method, and drug association was quantified. Among them, NS2 (1:4 β-CD: DPC) showed the highest loading efficiency (34.18% w/w). Variations in CUR loading reflected the influence of cross-linking density on complexation capacity. Due to its superior solubilization and loading efficiency, NS2 was selected for further studies.

DLS analysis revealed that CUNS exhibited an average particle size of 95–139 nm with a low PDI, indicating homogeneity. The high zeta potential confirmed complex stability and reduced agglomeration tendency. All formulations showed fine, free-flowing powder characteristics. TEM images confirmed spherical morphology and particle size consistent with DLS data, even after drug encapsulation.

FTIR spectra of β-CD, CDNS, CUR, their physical mixtures, and CURNS were analyzed. β-CD exhibited characteristic peaks at 3300–3400 cm^{-1} (O–H stretching), 2854 cm^{-1} (C–H stretching), and 1650 cm^{-1} (H–O–H bending). CDNS showed a carbonate bond peak at 1740–1750 cm^{-1}, confirming successful cross-linking, along with additional bands at 2918 cm^{-1} (C–H stretching), 1418 cm^{-1} (C–H bending), and 1026 cm^{-1} (C–O stretching). CU displayed peaks at 3450 cm^{-1} (phenolic O–H), 2850 cm^{-1} (C–H stretching), 1630 cm^{-1} (C=C), 1590 cm^{-1} (benzene ring), and 1510 cm^{-1} (C=O). In physical mixtures, bands from both components were observed, whereas in CUNS, spectral shifts and band modifications indicated molecular interactions and successful encapsulation of CU within the CDNS matrix.

XRD analysis confirmed the crystalline and amorphous nature of the studied components. β-CD exhibited sharp diffraction peaks at 2θ values of 7.5°, 12.2°, 15.7°, 17.6°, 19.3°, and 22.0°, reflecting its crystalline lattice. In contrast, CDNS showed a broad halo at 20–25°, indicative of an amorphous or partially crystalline structure due to molecular rearrangement during cross-linking. CUR displayed distinct crystalline peaks at 2θ values, such as 7.8°, 12.9°, 15.4°, 17.6°, and 26.6°, confirming its ordered crystalline nature. However, these peaks disappeared in the CUNS diffractogram, suggesting successful encapsulation of CUR within the CDNS matrix and conversion to an amorphous state.

DSC analysis of β-CD revealed a sharp endothermic peak at 290–300°C, confirming its melting point and thermal stability. In β-CD-based carbonate NS, an endothermic peak appeared at 50–100°C due to water loss, followed by no transitions until 350°C, indicating high thermal stability. An exothermic peak at 350–360°C corresponded to NS decomposition. CUR displayed a distinct endothermic peak at 176.57°C, attributable to its melting point, while physical mixtures retained the characteristic peaks of both components. In contrast, the CURNS thermogram showed the disappearance of CUR's melting peak and the presence of an exothermic event around 360°C, suggesting drug–carrier interactions, amorphization, or inclusion complex formation.

Buccal tablets – Formulation and evaluation

DOEs

Buccal tablet composition was optimized using experimental design and statistical analysis. RSM and the BBD were employed to evaluate critical formulation variables, their interactions, and their influence on tablet properties. A mathematical model was generated to determine optimal variable levels, minimizing the number of trial runs. This approach efficiently identified ideal tablet characteristics, resulting in an optimized buccal tablet formulation with enhanced performance and quality.

A BBD with 17 runs and a 3-factor, 3-level configuration was employed. Experimental results [Table 1] showed wide variations across responses: disintegration time in artificial saliva (Y1, 15.68–178.54 min), disintegration time in water (Y2, 3.42–169.24 min), swelling capacity (Y3, 1.76–9.23), time for 90% dissolution (Y4, 489.14–2097.33 min), peak detachment force (Y5, 0.43–4.32 N), and percentage permeability at 360 min (Y6, 1.34–16.38%). Data were fitted to a second-order quadratic model, whose suitability was confirmed through ANOVA, lack-of-fit tests, and R^2 values. High F-values [Table 2] validated the adequacy of the quadratic model for all response variables.

The polynomial equations describe the effects of independent variables on response variables, including main, interaction, and quadratic terms. Coefficient values indicate the magnitude and direction of these effects, with positive and negative signs representing synergistic and antagonistic influences, respectively. In orthogonal designs, the intercept corresponds to the mean response of all experimental runs. Model adequacy was assessed by comparing residual and pure errors through the lack-of-fit test. A non-significant lack of fit confirmed the predictive reliability of the quadratic models, all of which demonstrated good fitness.

The values of R^2, adjusted R^2, and coefficient of variation (CV) for all models were obtained using multiple linear regression analysis. All response variables exhibited R^2 values above 0.9922, confirming that the models explained the observed variability with high accuracy. Adjusted R^2 further validated model adequacy by accounting for the number of terms included, ensuring a more reliable assessment. The CV values for the six responses were 3.01, 4.56, 5.13, 2.72, 4.21, and 2.89, indicating low variability and high consistency of the experimental data.

Disintegration time in artificial saliva (Y_1)

Disintegration of buccal tablets in artificial saliva represents the breakdown of tablets in a simulated salivary environment, a critical parameter for assessing buccal drug delivery performance. The model exhibited high significance with an F-value of 432.50, indicating only a 0.01% chance of such a result arising from noise. Significant model terms included A, B, AB, AC, BC, A^2, B^2, and C^2, while terms with $P > 0.1000$ were considered non-significant and could be excluded to refine the model. The Predicted R^2 (0.9912) showed strong agreement with the Adjusted R^2 (0.9959), with a difference <0.2, confirming excellent model predictability. Adeq Precision, with a signal-to-noise ratio of 64.935, demonstrated adequate signal strength. Figure 1a shows strong agreement between predicted and observed Y1 values, while Figure 1b (perturbation plot) illustrates that increasing Carbopol® 934 (B) prolongs disintegration time. Equation 2 further reveals that A–B and A–C interactions positively influence Y1, whereas the B–C interaction is negative. Quadratic effects of A, B, and C were also significant at higher levels. Figure 1c-e present 3D response surface plots, highlighting these variable interactions.

$$Y_1 = 155.01 - 22.92\,A + 40.37\,B + 18.19\,AB + 5.14\,AC - 30.75\,BC - 50.90\,A^2 - 6.52\,B^2 - 40.65\,C^2 \quad (2)$$

Disintegration time in water (Y_2)

Disintegration facilitates drug release for absorption, ensuring therapeutic efficacy. Rapid tablet disintegration further enhances patient compliance by minimizing discomfort and the risk of choking. Therefore, evaluating buccal tablet disintegration in water is essential for developing effective and patient-friendly dosage forms. The model demonstrated strong significance, with an F-value of 256.80, indicating only a 0.01% probability of noise influencing the results.

Table 2: Statistical summary of response parameters

Source of variation	SS	DF	MSV	F-Value	*P*-value Prob>F	Source of variation	SS	DF	MSV	F-Value	*P*-value Prob>F
Disintegration time in artificial saliva (R1)						**Disintegration time in water (R2)**					
Model	41858.83	9	4650.98	432.5	<0.0001	Model	54711.29	9	6079.03	256.8	<0.0001
A	4203.53	1	4203.53	390.89	<0.0001	A	1726.37	1	1726.37	72.93	<0.0001
B	13034.67	1	13034.67	1212.1	<0.0001	B	18691.14	1	18691.14	789.58	<0.0001
AB	1323.14	1	1323.14	123.04	< 0.0001	C	989.9	1	989.9	41.82	0.0003
AC	105.78	1	105.78	9.84	0.0165	AB	571.93	1	571.93	24.16	0.0017
BC	3782.87	1	3782.87	351.77	< 0.0001	AC	149.21	1	149.21	6.3	0.0404
A^2	10910.28	1	10910.28	1014.55	<0.0001	BC	2983.34	1	2983.34	126.03	<0.0001
B^2	178.92	1	178.92	16.64	0.0047	A^2	12245.4	1	12245.4	517.29	<0.0001
C^2	6957.14	1	6957.14	646.95	<0.0001	B^2	853.92	1	853.92	36.07	0.0005
Residual	75.28	7	10.75			C^2	14120.77	1	14120.77	596.51	<0.0001
Lack of Fit	17.52	3	5.84	0.4045	0.7585	Residual	165.71	7	23.67		
Pure Error	57.75	4	14.44			Lack of Fit	106	3	35.33	2.37	0.2119
Cor Total	41934.1	16				Pure Error	59.71	4	14.93		
						Cor Total	54877	16			
Swelling capacity (R3)						**Time for 90% dissolution (R4)**					
Model	71.81	9	7.98	99.24	<0.0001	Model	2.97E+06	9	3.30E+05	285.71	<0.0001
A	19.22	1	19.22	239.05	<0.0001	A	1.18E+06	1	1.18E+06	1021.03	<0.0001
B	12.3	1	12.3	153	<0.0001	B	28561.7	1	28561.7	24.76	0.0016
C	38.54	1	38.54	479.41	<0.0001	C	2.12E+05	1	2.12E+05	183.37	<0.0001
AB	1.35	1	1.35	16.74	0.0046	AB	1.52E+05	1	1.52E+05	131.88	<0.0001
Residual	0.5628	7	0.0804			AC	69205.82	1	69205.82	60	0.0001
Lack of Fit	0.2122	3	0.0707	0.807	0.5521	B^2	92303.72	1	92303.72	80.03	<0.0001
Pure Error	0.3506	4	0.0877			C^2	1.27E+06	1	1.27E+06	1097.11	<0.0001
Cor Total	72.37	16				Residual	8073.71	7	1153.39		
						Lack of Fit	2715.42	3	905.14	0.6757	0.6108
						Pure Error	5358.3	4	1339.57		
						Cor Total	2.97E+06	16			
Peak detachment force (R5)						**Percent permeability at 360 min (R6)**					
Model	25.54	9	2.84	303.67	<0.0001	Model	371.24	9	41.25	602.49	<0.0001
A	0.078	1	0.078	8.35	0.0233	A	0.7938	1	0.7938	11.59	0.0114
B	0.1128	1	0.1128	12.07	0.0103	B	7.7	1	7.7	112.51	<0.0001
C	24.78	1	24.78	2652.18	<0.0001	C	359.25	1	359.25	5247.37	<0.0001
A^2	0.3847	1	0.3847	41.17	0.0004	C^2	2.87	1	2.87	41.93	0.0003
B^2	0.1178	1	0.1178	12.61	0.0093	Residual	0.4792	7	0.0685		
Residual	0.0654	7	0.0093			Lack of Fit	0.2523	3	0.0841	1.48	0.3466
Lack of Fit	0.0273	3	0.0091	0.9568	0.4941	Pure Error	0.2269	4	0.0567		
Pure Error	0.0381	4	0.0095			Cor Total	371.71	16			
Cor Total	25.6	16									

Significant model terms included A, B, C, AB, AC, BC, A^2, B^2, and C^2, while terms with $P > 0.1000$ were considered non-significant and could be excluded to refine the model. The Predicted R^2 (0.9674) closely matched the Adjusted R^2 (0.9931), with a difference <0.2, confirming robust predictability. Adeq Precision, with a Signal-to-Noise ratio (S/N ratio) of 41.588, further indicated adequate signal quality. A strong correlation between predicted and observed Y2 values was observed [Figure 2a]. The perturbation plot [Figure 2b] revealed that increasing Carbopol® 934 (B)

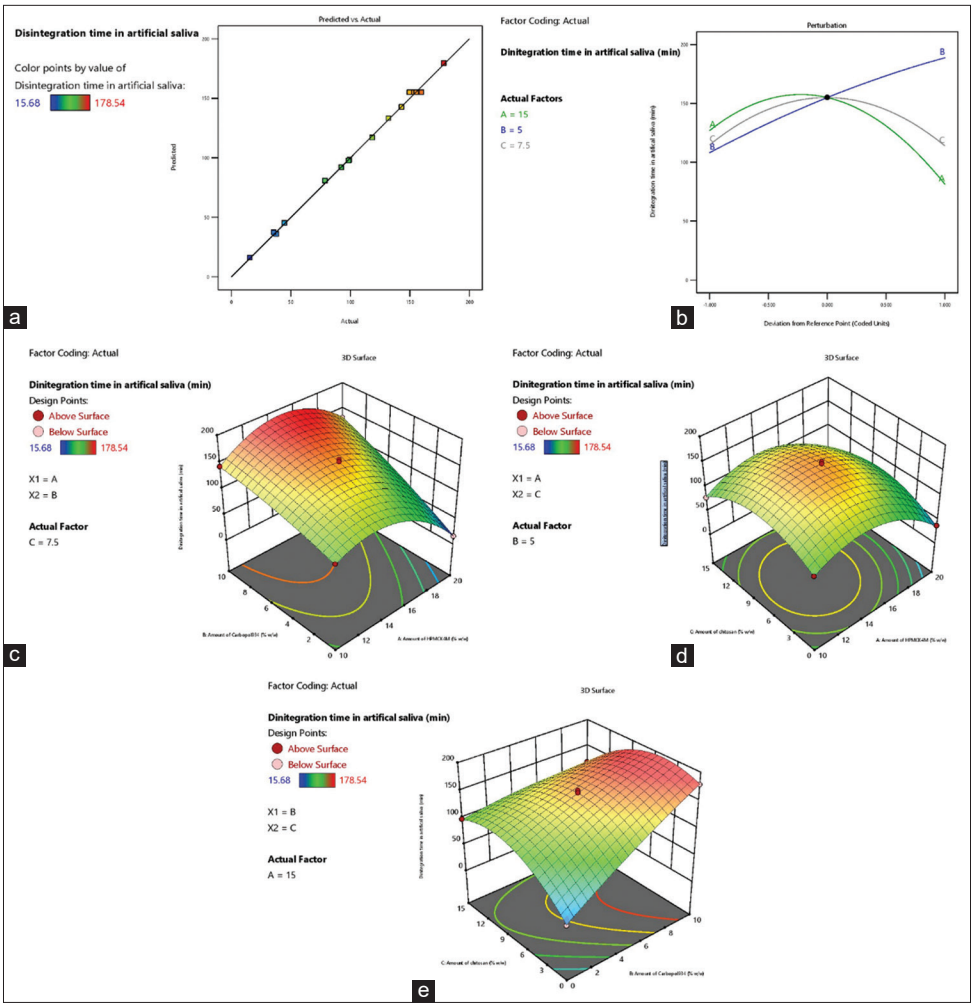

Figure 1: (a) Comparison between predicted and actual values of Y_1, (b) Perturbation plot showing the individual effect of individual variables on Y_1, (c) 3-D response surface plot showing the interactive effect of A and B on Y_1, (d) 3-D response surface plot showing the interactive effect of A and C on Y_1, (e) 3-D response surface plot showing the interactive effect of B and C on Y_1

extended disintegration time, while Equation 3 showed positive interactive effects for A–B and A–C, and a negative effect for B–C. At higher concentrations, all three factors (A, B, and C) exhibited significant quadratic effects. Response surface plots [Figure 2c-e] further illustrated these interactions.

$$Y_2 = 166.05 - 14.69 + 48.34\ B + 11.12\ C + 11.96\ AB + 6.11\ AC - 27.31\ BC - 53.93\ A^2 - 14.24\ B^2 - 57.91\ C^2 \quad (3)$$

Swelling capacity (Y_3)

Swelling capacity refers to the ability of buccal tablets to absorb and retain fluids, forming a gel-like layer that prolongs drug release and enhances contact with the buccal mucosa. This property is critical for improving bioavailability and therapeutic efficacy. The model was highly significant, with an F-value of 99.24, suggesting only a 0.01% probability of noise interference. Significant model terms included A, B, C, and AB, while terms with $P > 0.1000$ were deemed non-significant and could be excluded for refinement. The Predicted R^2 (0.9455) is closely aligned with the Adjusted R^2 (0.9822), with a difference <0.2, confirming strong predictability. Adeq Precision, with an S/N ratio of 34.441, further indicated adequate signal quality. A strong correlation between predicted and observed Y3 values was observed [Figure 3a]. The perturbation plot [Figure 3b] demonstrated that A, B, and C positively influenced swelling capacity, whereas Equation 4 indicated a negative interaction between A and B. The 3D response surface plot [Figure 3c] illustrated the interactive effects of A and B on Y3.

$$Y_3 = 5.43 + 1.55\ A + 1.24\ B + 2.20\ C - 0.58\ AB \quad (4)$$

Time for 90% dissolution (Y_4)

The time required for 90% drug dissolution (T90%) is a critical parameter for evaluating the release profile and performance of buccal tablets. The model was highly significant, with an F-value of 285.71, indicating only a 0.01% probability of noise interference. Significant model terms included A, B, C, AB, AC, B^2, and C^2, while those with $P > 0.1000$ were considered non-significant. The Predicted R^2 (0.9826) is closely matched the Adjusted R^2 (0.9938), with a difference

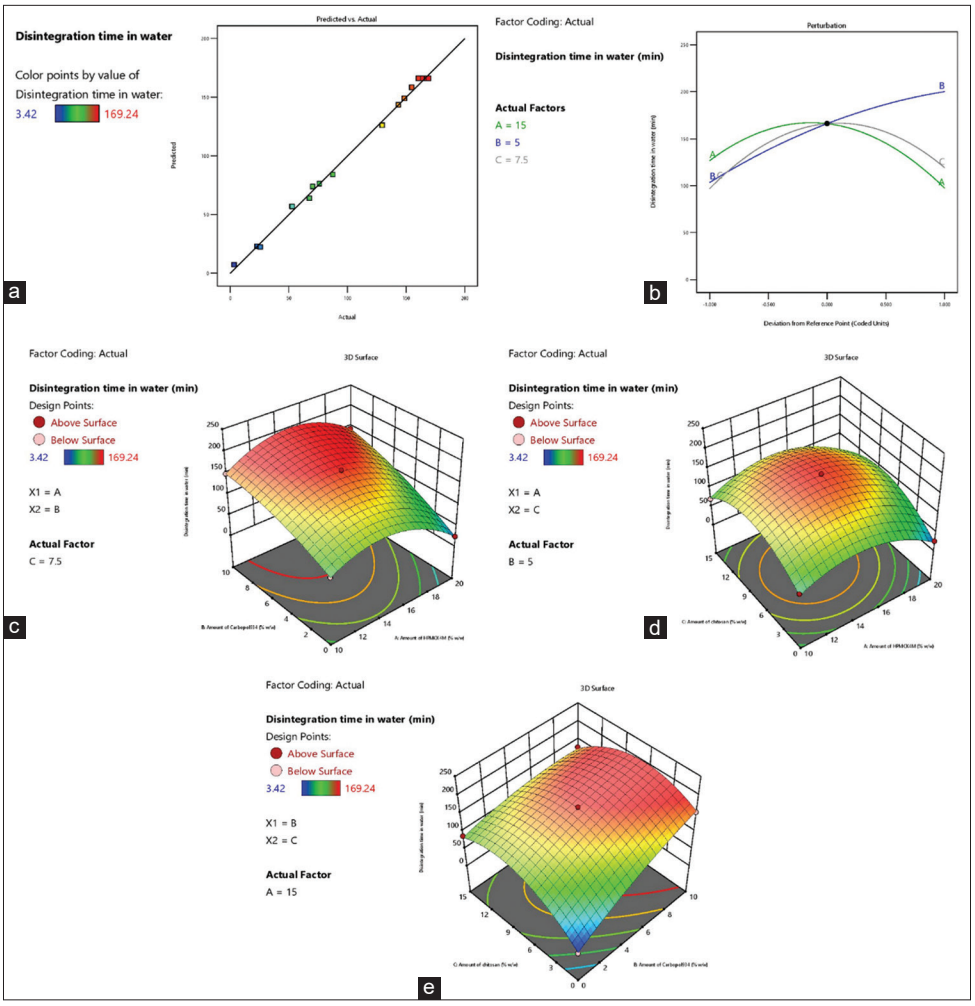

Figure 2: (a) Comparison between predicted and actual values of Y_2, (b) Perturbation plot showing the individual effect of individual variables on Y_2, (c) 3-D response surface plot showing the interactive effect of A and B on Y_2, (d) 3-D response surface plot showing the interactive effect of A and C on Y_2, (e) 3-D response surface plot showing the interactive effect of B and C on Y_2

<0.2, confirming model reliability. Adeq Precision, with an S/N ratio of 62.576, indicated an adequate signal. A strong correlation was observed between predicted and experimental values of Y4 [Figure 4a]. The perturbation plot [Figure 4b] revealed that factors A and B negatively influenced T90%, while factor C exerted a positive effect, with higher C levels increasing dissolution and higher A and B levels reducing it. Equation 5 confirmed negative interactive effects between A–B and A–C, while quadratic effects of B and C were also significant. The 3D response surface plots [Figure 4c and d] illustrated these interactions.

$$Y_4 = 1431.30 - 383.67\,A - 59.75\,B + 162.60\,C - 195\,AB - 131.54\,AC + 148.06\,B^2 - 548.21\,C^2 \quad (5)$$

Peak detachment force (Y_5)

The peak detachment force represents the maximum force required to detach buccal tablets from the mucosal surface, indicating their adhesive strength. The model was highly significant (F = 303.67), with only a 0.01% chance of the result arising from noise. Significant terms included A, B, C, A^2, and B^2, while non-significant terms ($P > 0.1000$) were excluded. Predicted R^2 (0.9806) closely matched Adjusted R^2 (0.9942), and Adeq Precision (S/N ratio 51.425) confirmed a sufficient signal. Perturbation analysis showed that factors A and B negatively influenced Y5, whereas C had a positive effect. The peak detachment force increased with higher C concentration but decreased with higher A and B levels, and quadratic effects of A and B were significant, as shown in Equation 6.

$$Y_5 = 2.49 - 0.09\,A - 0.11\,B + 1.76\,C - 0.30\,A^2 - 0.16\,B^2 \quad (6)$$

Percent permeability at 360 min (Y_6)

Percent permeability (Y6) represents the fraction of drug that passes through the buccal mucosa and becomes systemically available, reflecting the extent of buccal absorption over time. The model was highly significant (F = 602.49), with only a 0.01% probability of the result arising from noise. Significant terms included A, B, C, and C^2, while non-significant terms ($P > 0.1000$) were excluded. Predicted R^2 (0.9882) closely matched Adjusted R^2 (0.9971), and Adeq Precision (S/N

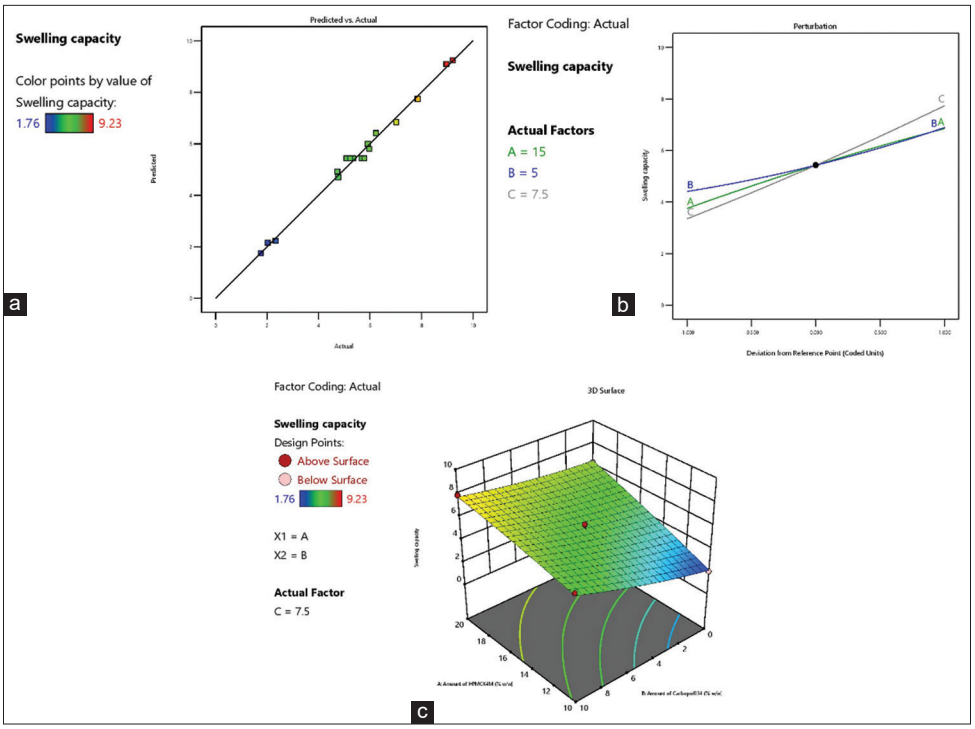

Figure 3: (a) Comparison between predicted and actual values of Y_3, (b) Perturbation plot showing the individual effect of individual variables on Y_3, (c) 3-D response surface plot showing the interactive effect of A and B on Y_3

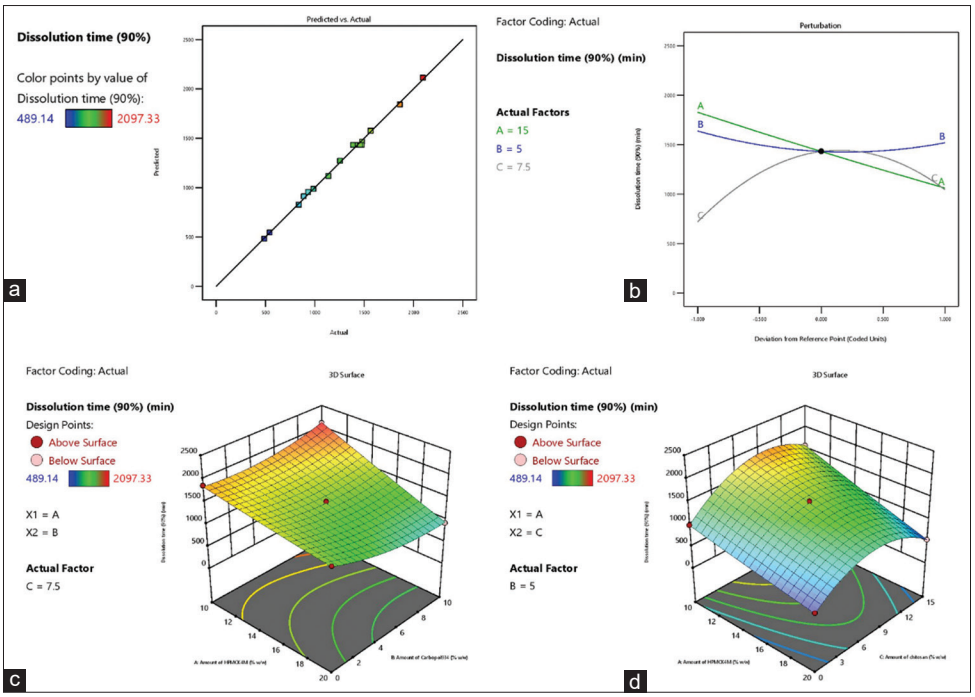

Figure 4: (a) Comparison between predicted and actual values of Y_4, (b) Perturbation plot showing the individual effect of individual variables on Y_4, (c) 3-D response surface plot showing the interactive effect of A and B on Y_4, (d) 3-D response surface plot showing the interactive effect of A and C on Y_4

ratio 76.564) confirmed adequate signal quality. Perturbation analysis [Figure 6b] indicated that B and C positively influenced permeability, whereas A had a negative effect. Permeability increased with higher B and C concentrations but decreased with increasing A. In addition, C exhibited significant quadratic effects, as shown in Equation 7.

$$Y_6 = 9.56 - 0.31\,A + 0.98\,B + 6.70\,C - 0.82\,C^2 \quad (7)$$

The optimal levels of critical formulation variables HPMC® K4M (A), Carbopol® 934 (B), and Chitosan (C) affecting Y1–Y6 were determined using numerical optimization with defined desirability constraints. Predicted and observed

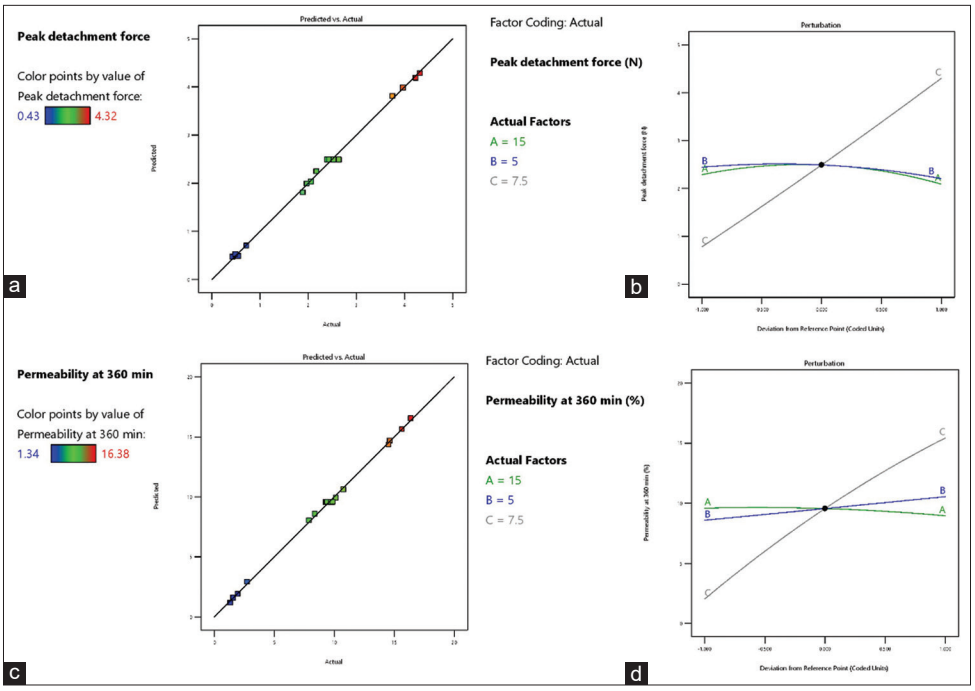

Figure 5: (a) Comparison between predicted and actual values of Y_5, (b) Perturbation plot showing the individual effect of individual variables on Y_5, (c) Comparison between predicted and actual values of Y_6, (d) Perturbation plot showing the individual effect of individual variables on Y_6

responses at these optimal levels are presented in Figure 6a. Figure 6b shows the overlay plot of the design space for factors and responses, achieving a desirability of 0.814. A control strategy was implemented by selecting formulation variables within this design space to ensure robust and consistent results. The optimized formulation comprised 16.59% w/w HPMC® K4M, 9.91% w/w Carbopol® 934, and 14.49% w/w Chitosan. The reliability of the optimization was confirmed through three confirmatory experiments (T1–T3), with observed responses closely matching the predicted values, as shown in Figure 6c.

Buccal tablets evaluation

The CURNS buccal tablets were prepared through direct compression by blending the specified excipients and compressing them into tablets. The prepared tablets were stored in amber-colored containers and evaluated for quality control parameters. Tablet weight ranged from 299.25 to 301.84 mg, thickness from 4.85 to 5.18 mm, hardness from 5.04 to 5.39 kg/cm^2, and friability from 0.48 to 0.78%. The drug content was 98.44–99.61%.

Among the formulations, T3 exhibited the highest swelling index. The tablet pH ranged from 6.7 to 6.8, falling within the normal salivary pH range (5–7). Mucoadhesion values were 18.37 g, 20.83 g, and 21.25 g, primarily influenced by the mucoadhesive polymer properties. The buccal residence time ranged from 6.2 to 6.8 h, reflecting the duration the tablets remained attached to the mucosa.

In vitro release study

Pure CUR powder exhibited a slow release profile, with only ~29% drug released over 24 h and ~15.5% released within the first 2 h. In contrast, both CURNS powder and CURNS buccal tablets showed similar biphasic release patterns, with an initial rapid release of ~23% in the first 2 h, followed by sustained release over 24 h, ultimately achieving ~99% drug release at the end of the period.

Drug release kinetic analysis

The drug release data from the formulated buccal tablets were analyzed using mathematical models – zero-order, first-order, Higuchi, and Korsmeyer-Peppas – to understand the release behavior. Model fitting was evaluated using the coefficient of determination (R^2), with values closer to 1 indicating better correlation. The first-order model showed the highest correlation (R^2 = 0.9911), followed by Korsmeyer-Peppas (R^2 = 0.9398), Higuchi (R^2 = 0.9171), and zero-order (R^2 = 0.7585), indicating that the drug release primarily followed first-order kinetics. In addition, the Korsmeyer-Peppas model was applied to elucidate the release mechanism, which indicated Super Case II transport as the release exponent (n) was less than 0.89.

Stability study

Stability studies were conducted by storing the tablets under both accelerated (high temperature and humidity) and real-time (ambient) conditions. Periodic assessments of

Factors

	Factor	Name	Level	Low Level	High Level	Std. Dev.	Coding
	A	Amount of HPMCK4M	16.59	10.00	20.00	0.0000	Actual
	B	Amount of Carbopol934	9.91	0.0000	10.00	0.0000	Actual
	C	Amount of chitosan	14.49	0.0000	15.00	0.0000	Actual

Point Prediction

Point Prediction

Two-sided Confidence = 95% Population = 99%

Solution 1 of 7 Response	Predicted Mean	Predicted Median	Observed	Std Dev	SE Mean	95% CI low for Mean	95% CI high for Mean	95% TI low for 99% Pop	95% TI high for 99% Pop
Dinitegration time in artifical saliva	119.25	119.25		3.2793	2.71865	112.821	125.678	98.9187	139.581
Disintegration time in water	130.289	130.289		4.86542	4.0336	120.751	139.827	100.125	160.454
Swelling capacity	9.22996	9.22996		0.283549	0.235072	8.6741	9.78582	7.47201	10.9879
Dissolution time (90%)	954.836	954.836		33.9616	28.1553	888.259	1021.41	744.28	1165.39
Peak detachment force	3.78425	3.78425		0.0966622	0.0801362	3.59476	3.97374	3.18496	4.38354
Permeability at 360 min	15.9815	15.9815		0.261655	0.216921	15.4686	16.4944	14.3593	17.6037

a

Factor Coding: Actual

Overlay Plot

Dinitegration time in artifical saliva
Disintegration time in water
Swelling capacity
Dissolution time (90%)
Peak detachment force
Permeability at 360 min

X1 = A
X2 = B

Actual Factor

C = 14.4893

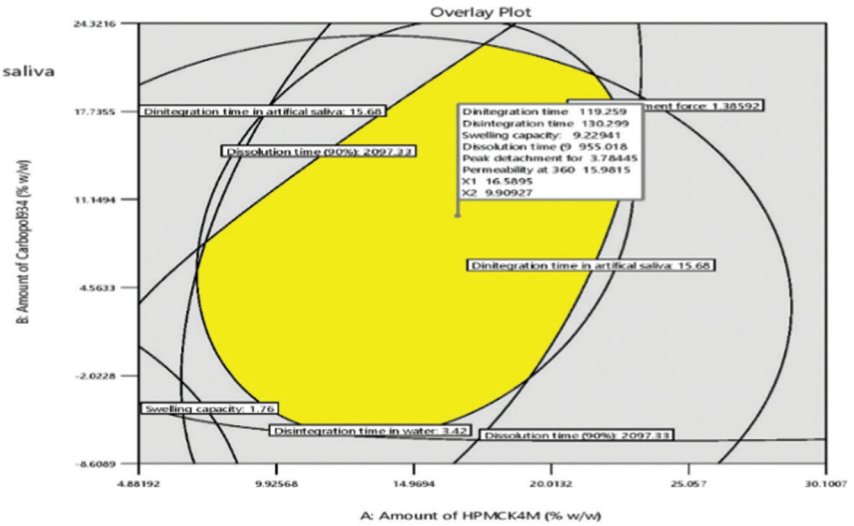

b

Confirmation Location #1

Amount of HPMCK4M	Amount of Carbopol934	Amount of chitosan
16.5838	9.90674	14.4952

Response data

Runs: 3

Dinitegration time in artifical saliva	Disintegration time in water	Swelling capacity	Dissolution time (90%)	Peak detachment force	Permeability at 360 min
118.56	127.67	9.34	986.54	3.97	15.78
120.63	132.85	8.95	1034.38	3.85	16.43
126.34	140.32	9.76	923.43	3.65	16.28

Confirmation

Confirmation

Two-sided Confidence = 95%

Analysis	Predicted Mean	Predicted Median	Observed	Std Dev	n	SE Pred	95% PI low	Data Mean	95% PI high
Dinitegration time in artifical saliva	119.202	119.202		3.2793	3	3.31292	111.368	121.843	127.035
Disintegration time in water	130.23	130.23		4.86542	3	4.91529	118.607	133.613	141.852
Swelling capacity	9.22999	9.22999		0.283549	3	0.286455	8.55263	9.35	9.90735
Dissolution time (90%)	954.817	954.817		33.9616	3	34.3097	873.688	981.45	1035.95
Peak detachment force	3.78633	3.78633		0.0966622	3	0.097653	3.55542	3.82333	4.01724
Permeability at 360 min	15.9858	15.9858		0.261655	3	0.264338	15.3608	16.1633	16.6109

c

Figure 6: (a) The optimum levels of formulation variables and predicted values of response variables, (b) Overlay plot showing the design space, (c) Results of the confirmation experiments

appearance, disintegration time (DT), drug content, and drug release (DR) were performed. The results showed that the tablets remained stable throughout the study period, with no significant changes in appearance, hardness, DT, dissolution, or drug content.

SUMMARY

This research details the design and evaluation of a mesoporous CDNS-based buccal delivery system for curcumin, targeting improvements in solubility, stability, and

therapeutic efficacy. CDNS were prepared through cross-linking and loaded with CUR using freeze-drying. Buccal tablets were developed through direct compression and optimized using a BBD. The optimized formulation exhibited favorable physicochemical properties, strong mucoadhesion, and compatibility with the buccal mucosa. *In vitro* studies demonstrated a biphasic, sustained release of CUR, with up to 99% release over 24 h. Stability assessments confirmed the formulation's robustness. Overall, mesoporous CDNS-based buccal systems represent a promising approach for enhancing the delivery of poorly soluble drugs, such as curcumin.

CONCLUSION

This study highlights mesoporous CDNSs as a promising platform for buccal delivery of curcumin. CDNS were prepared through cross-linking and efficiently loaded with CUR using freeze-drying. Buccal tablets, formulated by direct compression and optimized through a BBD, exhibited favorable physicochemical properties, high swelling, and salivary-compatible surface pH. Both CURNS powder and tablets showed a biphasic release, with ~99% drug release over 24 h, supporting enhanced therapeutic efficacy and reduced dosing frequency. Stability studies confirmed the formulation's robustness, demonstrating that CDNS-based buccal tablets offer sustained release, good stability, and an effective strategy for delivering poorly soluble drugs, such as curcumin.

AUTHOR'S CONTRIBUTIONS

The contributions from each author are equal.

ACKNOWLEDGMENT

The authors gratefully acknowledge the Department of Pharmaceutical Sciences, Jawaharlal Nehru Technological University, Ananthapuramu, and Ratnam Institute of Pharmacy, Pidathapolur, Nellore, Andhra Pradesh, India, for providing the facilities necessary to carry out this research.

FUNDING

Not applicable.

REFERENCES

1. Dei Cas M, Ghidoni R. Dietary curcumin: Correlation between bioavailability and health potential. Nutrients 2019;11:2147.
2. Dizaj SM, Alipour M, Abdolahinia ED, Ahmadian E, Eftekhari A, Forouhandeh H, *et al*. Curcumin nanoformulations: Beneficial nanomedicine against cancer. Phytother Res 2022;36:1156-81.
3. Obeid MA, Alsaadi M, Aljabali AA. Recent updates in curcumin delivery. J Liposome Res 2023;33:53-64.
4. Ma Z, Wang N, He H, Tang X. Pharmaceutical strategies of improving oral systemic bioavailability of curcumin for clinical application. J Control Release 2019;316:359-80.
5. Han HS, Koo SY, Choi KY. Emerging nanoformulation strategies for phytocompounds and applications from drug delivery to phototherapy to imaging. Bioact Mater 2022;14:182-205.
6. Wang Q, Zhang A, Zhu L, Yang X, Fang G, Tang B. Cyclodextrin-based ocular drug delivery systems: A comprehensive review. Coord Chem Rev 2023;476:214919.
7. Real DA, Bolaños K, Priotti J, Yutronic N, Kogan MJ, Sierpe R, *et al*. Cyclodextrin-modified nanomaterials for drug delivery: Classification and advances in controlled release and bioavailability. Pharmaceutics 2021;13:2131.
8. Reddy KS, Bhikshapathi D, Kumar JP. Unlocking dabrafenib's potential: A quality by design (QbD) journey to enhance permeation and oral bioavailability through nanosponge formulation. Braz J Pharm Sci 2025;61:e24209.
9. Reddy KS, Bhikshapathi D. Design and optimization of DPC-crosslinked HPβCD nanosponges for entrectinib oral delivery: Formulation, characterization, and pharmacokinetic studies. Future J Pharm Sci 2024;10:101.
10. Selvamuthukumar S, Anandam S, Krishnamoorthy K, Rajappan M. Nanosponges: A novel class of drug delivery system-review. J Pharm Pharm Sci 2012;15:103-11.
11. Anandam S, Selvamuthukumar S. Fabrication of cyclodextrin nanosponges for quercetin delivery: Physicochemical characterization, photostability, and antioxidant effects. J Mater Sci 2014;49:8140-53.
12. Gholibegloo E, Mortezazadeh T, Salehian F, Ramazani A, Amanlou M, Khoobi M. Improved curcumin loading, release, solubility and toxicity by tuning the molar ratio of cross-linker to β-cyclodextrin. Carbohydr Polym 2019;213:70-8.
13. Singh P, Ren X, Guo T, Wu L, Shakya S, He Y, *et al*. Biofunctionalization of β-Cyclodextrin nanosponges using cholesterol. Carbohydr Polym 2018;190:23-30.
14. Hoti G, Appleton SL, Rubin Pedrazzo A, Cecone C, Matencio A, Trotta F, *et al.* Strategies to develop cyclodextrin-based nanosponges for smart drug delivery. In: Smart Drug Delivery. London: IntechOpen; 2021.
15. Swaminathan S, Vavia PR, Trotta F, Cavalli R. Nanosponges encapsulating dexamethasone for ocular delivery: Formulation design, physicochemical characterization, safety and corneal permeability assessment. J Biomed Nanotechnol 2013;9:998-1007.
16. Pawar S, Shende P, Trotta F. Diversity of β-cyclodextrin-based nanosponges for the transformation of actives. Int

J Pharm 2019;565:333-50.
17. Nguyen OO, Tran KD, Ha NT, Doan SM, Dinh TT, Tran H. Oral cavity: An open horizon for nanopharmaceuticals. J Pharm Investig 2021;51:413-24.
18. Jana BK, Singh M, Dutta RS, Mazumder B. Current drug delivery strategies for buccal cavity ailments using mouth dissolving wafer technology: A comprehensive review on the present state of the art. Curr Drug Deliv 2024;21:339-59.
19. Hua S. Advances in nanoparticulate drug delivery approaches for sublingual and buccal administration. Front Pharmacol 2019;10:1328.
20. Macedo AS, Castro PM, Roque L, Thome MG, Reis CP, Pintado ME, *et al*. Novel and revisited approaches in nanoparticle systems for buccal drug delivery. J Control Release 2020;320:125-41.
21. Lam JK, Cheung CC, Chow MY, Harrop E, Lapwood S, Barclay SI, *et al*. Transmucosal drug administration as an alternative route in palliative and end-of-life care during the COVID-19 pandemic. Adv Drug Deliv Rev 2020;160:234-43.
22. Lou J, Duan H, Qin Q, Teng Z, Gan F, Zhou X, *et al*. Advances in oral drug delivery systems: Challenges and opportunities. Pharmaceutics 2023;15:484.
23. Gowthamarajan K, Jawahar N, Prashant W, Kunal J, Sumeet S. Development of buccal tablets for curcumin using *Anacardium occidentale* gum. Carbohydr Polym 2012;88:1177-83.
24. Mazzarino L, Borsali R, Lemos-Senna E. Mucoadhesive films containing chitosan-coated nanoparticles: A new strategy for buccal curcumin release. J Pharm Sci 2014;103:3764-71.
25. Liu Z, Smart JD, Pannala AS. Recent developments in formulation design for improving oral bioavailability of curcumin: A review. J Drug Deliv Sci Technol 2020;60:102082.
26. Brady J, Dürig T, Lee PI, Li JX. Polymer properties and characterization. In: Developing Solid Oral Dosage Forms. 2nd ed. United States: Academic Press; 2017.
27. Mansuri S, Kesharwani P, Jain K, Tekade RK, Jain NK. Mucoadhesion: A promising approach in drug delivery system. React Funct Polym 2016;100:151-72.
28. Sethi S, Mangla B, Kamboj S, Rana V. A QbD approach for the fabrication of immediate and prolong buoyant cinnarizine tablet using polyacrylamide-g-corn fiber gum. Int J Biol Macromol 2018;117:350-61.
29. Vigani B, Rossi S, Sandri G, Bonferoni MC, Caramella CM, Ferrari F. Recent advances in the development of *in situ* gelling drug delivery systems for non-parenteral administration routes. Pharmaceutics 2020;12:859.
30. Ugoeze KC. Bioadhesive polymers for drug delivery applications. In: Bioadhesives in Drug Delivery. Boca Raton: CRC Press; 2020.
31. Irimia T, Ghica MV, Popa L, Anuţa V, Arsene AL, Dinu-Pirvu CE. Strategies for improving ocular drug bioavailability and corneal wound healing with chitosan-based delivery systems. Polymers 2018;10:1221.
32. Singireddy A, Subramanian S. Cyclodextrin nanosponges to enhance the dissolution profile of quercetin by inclusion complex formation. Part Sci Technol 2016;34:341-6.
33. Pedireddi S, Singireddy A, Varma MM, Jayanthi VR. Differential properties of nanoporous nanosponges prepared from β-cyclodextrin and 2-hydroxypropyl β-cyclodextrin. Adv Sci Eng Med 2019;1:823-35.
34. Singireddy A, Pedireddi SR, Subramanian S. Optimization of reaction parameters for the synthesis of cyclodextrin nanosponges in controlled nanoscopic size dimensions. J Polym Res 2019;26:93.
35. Anandam S, Selvamuthukumar S. Optimization of microwave-assisted synthesis of cyclodextrin nanosponges using response surface methodology. J Porous Mater 2014;21:1015-23.
36. Li H, van den Driesche S, Bunge F, Yang B, Vellekoop MJ. Optimization of on-chip bacterial culture conditions using the Box-Behnken design response surface methodology for faster drug susceptibility screening. Talanta 2019;194:627-33.
37. Agbovi HK, Wilson LD. Flocculation optimization of orthophosphate with FeCl3 and alginate using the Box-Behnken response surface methodology. Ind Eng Chem Res 2017;56:3145-55.
38. Perrone M, Lopalco A, Lopedota A, Cutrignelli A, Laquintana V, Franco M, *et al*. S-preactivated thiolated glycol chitosan useful to combine mucoadhesion and drug delivery. Eur J Pharm Biopharm 2018;132:103-11.
39. Koirala S, Nepal P, Ghimire G, Basnet R, Rawar I, Dahal A, *et al*. Formulation and evaluation of mucoadhesive buccal tablets of aceclofenac. Heliyon 2021;7:e06439.
40. Mehrabi F, Shamspur T, Mostafavi A, Hakimi H, Mohamadi M. Inclusion of sulfamethoxazole in a novel CuFe2O4 nanoparticles/mesoporous silica-based nanocomposite: Release kinetics and antibacterial activity. Appl Organomet Chem 2021;35:e6035.
41. Modi S, Anderson BD. Determination of drug release kinetics from nanoparticles: Overcoming pitfalls of the dynamic dialysis method. Mol Pharm 2013;10: 3076-89.
42. Singireddy A, Pedireddi SR, Nimmagadda S, Selvamuthukumar S. Beneficial effects of microwave-assisted heating versus conventional heating in the synthesis of cyclodextrin-based nanosponges. Mater Today Proc 2016;3:3951-9.

Source of Support: Nil. **Conflicts of Interest:** None declared.